Chapter 1

Introduction: DNA Signaling by Iron-Sulfur Cluster Proteins

Adapted from: Bartels, P.L.; O'Brien, E.; Barton, J.K. DNA Signaling by Iron-Sulfur Cluster Proteins. pp. 405 – 423 in *Iron-Sulfur Clusters in Chemistry and Biology, 2nd ed.* (ed. Rouault, T.), DeGruyter, Berlin/Boston.

[4Fe4S] Clusters in DNA Processing Enzymes and DNA Charge Transport

The multi-metal [4Fe4S] clusters in mitochondrial and cytosolic proteins have long been known to serve critical functions ranging from electron transfer to catalysis (*1*). In an exciting turn, the last three decades have expanded the known cellular distribution of [4Fe4S] clusters to the nucleus, where they occur in DNA-processing enzymes throughout all domains of life (*2-12*). **Table 1.1** illustrates many of these new DNA processing enzymes containing [4Fe4S] clusters. As is evident from the table, [4Fe4S] clusters occur in proteins involved in all aspects of DNA processing. These enzymes are structurally and functionally diverse, acting in a range of pathways from base excision repair (BER) and nucleotide excision repair (NER) to DNA replication. Many of these proteins are known to be disease relevant, and so determining the function of the cluster has been a high priority (*13, 14*). In all of these proteins, the [4Fe4S] cluster is non-catalytic and largely redox-inert in solution, and only secondarily involved in maintaining structural integrity (*15, 16*). Despite some evidence to the contrary and the metabolic expense of inserting such a complex cofactor (*15 -17*), the cluster was typically assigned a structural role. This area remained highly contentious for years, but work in the Barton lab has demonstrated that DNA binding activates these proteins toward redox chemistry through an electrostatically-induced potential shift (*18*). The activation of these proteins for redox activity when bound to DNA enables them to take advantage of a fundamental property of DNA known as DNA charge transport (DNA CT).

DNA CT involves the transport of electrons or holes through the π-stacked base pairs; this process remains functional over long distances as long as stacking is not perturbed (i.e., by lesions, mismatches, or proteins that sharply kink the DNA) (*18*). Indeed, the sensitivity of DNA CT as a damage reporter led to much interest in possible biological applications of DNA CT, and

sparked initial interest in studying the mysterious [4Fe4S] proteins. The connection between [4Fe4S] proteins and DNA CT has proven to be extraordinarily fruitful from both perspectives. Over the course of numerous studies described later in this chapter, DNA CT has been found to help [4Fe4S] proteins search the genome for damage in a timely manner and to coordinate their activities by long-range redox signaling. The development of this model has since begun to provide insight into a range of poorly-understood mutations in the [4Fe4S] domain of repair proteins, and the importance of signaling among these proteins to disease-causing mutations underscores the need for a better understanding of the chemistry of [4Fe4S] clusters in DNA processing (*8,13,14*).

Until recently, the study of [4Fe4S] proteins was largely limited to bacterial repair proteins, with the behavior of their eukaryotic counterparts assumed to be similar. The work described in Chapters 2 and 3 describes some additional experiments to clarify details regarding bacterial repair proteins, while Chapter 4 discusses the first investigation of DNA CT in one of the eukaryotic homologues of bacterial BER proteins, human MUTYH. In addition, it has only recently become apparent that [4Fe4S] clusters are not uncommon in eukaryotic DNA replication proteins, and these include DNA primase and the B-family DNA polymerases. Chapters 5 through 7 describe multiple approaches to the study of one of these enzymes, the yeast lagging strand polymerase, DNA polymerase (Pol) δ. With the realization that [4Fe4S] proteins utilize DNA CT, it also became interesting to see if the single-stranded binding protein RPA could facilitate CT on ssDNA and serve to expand the possible signaling routes of redox-active proteins. Preliminary work with RPA thus constitutes Chapter 8. In this chapter, an outline of the studies that led to the current model for redox signaling in DNA repair is provided along with the

developments that led to an expansion and generalization of the model to include DNA replication proteins.

Table 1.1 DNA-processing [4Fe4S] proteins from the 3 domains of life.

Pathway	[4Fe4S] Proteins			Function
	Bacteria	Archaea	Eukarya	
Base Excision Repair (BER)	EndoIII, MutY	UDG, Mig	Ntg2, MUTYH, DME	DNA glycosylases that excise oxidized or misincorporated bases
Nucleotide Excision Repair (NER)	-	XPD	Rad3/XPD	Helicases that unwind DNA surrounding bulky lesions
DNA Replication	-	-	DNA Primase, DNA Polymerase (Pol) α, δ, ε, ζ	RNA priming of ssDNA and 5' - 3' synthesis of primed DNA
Replication Coupled Repair	AddAB, DinG	-	Dna2, FANCJ, ExoV	Varied; helicases and nucleases that expose ssDNA for homologous recombination or, in the case of DinG, unwind R-loops
Telomere Maintenance/Meiotic Crossover	-	-	Rtel1, Chl1	Helicases that unwind specialized DNA structures
Transcription	-	RNA Polymerase	Elp3	Template-directed RNA synthesis

DNA-Mediated Signaling in Base Excision Repair

The BER pathway involves the targeting and removal of damaged or misincorporated bases from DNA by one of several specialized DNA glycosylase enzymes (*2*). The resulting abasic (AP) site is then exposed by an endonuclease that nicks the phosphate backbone, allowing the short gap to be filled in by a DNA polymerase and then sealed by a DNA ligase. Within this pathway, [4Fe4S] clusters are present in several glycosylases of the helix-hairpin-helix family; the *Escherichia coli* enzymes endonuclease III (EndoIII) and MutY were the first well-characterized examples (*3-6*). EndoIII is a bifunctional glycosylase responsible for excising oxidized pyrimidines and nicking the DNA backbone at the site of damage, while MutY is a monofunctional glycosylase that removes adenine mispaired with 8-oxoguanine. Homologues of both proteins are present in nearly all organisms, from bacteria to man, and the [4Fe4S] domain is conserved throughout (*4, 6*). Early studies on EndoIII by Cunningham showed the cluster to be largely insensitive to both oxidation and reduction, leading to the eventual assignment of a structural role (*3, 15*). In the case of MutY, however, the cluster was found to be unnecessary for structural integrity, and a possible substrate-sensing role for the cluster was proposed instead (*5*). However, this mechanism could not explain the role of the [4Fe4S] cluster in proteins other than MutY, and recent work demonstrating full activity in the MutY homologues of anaerobic organisms that lack a cluster entirely provides a further argument against this possibility (*16*). Amidst this perplexing situation, support for a functional role for the cluster arose, due to strict conservation of [4Fe4S] clusters in these proteins despite the metabolic expense associated with cluster production and loading into target apoproteins (*17*).

Unexpectedly, the key to understanding the role of the cluster turned out to be a fundamental property of the DNA substrate itself: ground state B-form DNA can conduct charge

due to the π-stacked arrangement of the aromatic base pairs, which have a similar spacing and arrangement to that of conductive graphite sheets (*18*). This remarkable property was demonstrated in the ground state through electrochemical experiments where DNA containing a covalent alkane-thiol linker at one end was tethered to a gold electrode, and a redox-active intercalator appended to the opposite end of the duplex served as an electron donor/acceptor upon the application of a potential (Figure 1.1). Using cyclic voltammetry (CV) and square wave voltammetry (SQWV), rapid, long-range charge transport (CT) has been observed over distances up to 34nm (100bp of duplex DNA) with rates comparable to those measured in a 17-mer (*19*). CT is efficient even with multiple breaks present in the phosphate backbone, but just a slight perturbation to base stacking, such as the presence of a CA mismatch, has been shown to sharply attenuate charge transport yields (Figure 1.1). Well-stacked base pairs are thus a requirement for DNA CT. The biological accessibility of DNA on this platform has been demonstrated by experiments measuring restriction enzyme activity electrochemically, so that proteins are able to recognize their cognate sequence and carry out reactions on the DNA duplex on the electrode. Overall, CT renders DNA an effective redox sensor of DNA integrity in cells, and this concept, combined with the propensity of biological systems to use all available resources at their disposal, led to a series of experiments designed to test the redox activity of DNA-bound [4Fe4S] proteins.

To determine if otherwise redox-inert [4Fe4S] proteins could become activated to carry out DNA CT upon binding the DNA polyanion, [4Fe4S] proteins were added to DNA-modified gold electrodes, with the DNA-bound [4Fe4S] enzyme taking the place of a redox probe (Figure 1.2). In a revealing study, EndoIII and MutY from *E. coli* and Uracil DNA glycosylase (UDG) from *Archeoglobus fulgidus* were each incubated in buffered solution at physiological pH on

DNA-modified electrodes and scanned by CV (*20*). Remarkably, a reversible redox signal was observed for all three proteins and at quite similar potentials. DNA CT from the protein to electrode surface was severely attenuated both in the absence of DNA and when the DNA duplex contained an intervening abasic site proximal to the electrode surface, verifying that the signal was DNA-mediated. Midpoint potentials ranging from 75 mV versus NHE (EndoIII) to 95 mV (MutY and UDG) placed all three enzymes at the lower end of the 100-300 mV range reported for high potential iron proteins (HiPIPs), and well above the -200 to -600 mV range expected for ferredoxins (*21*). These electrochemical results, combined with data from EPR spectroscopy of native and chemically oxidized DNA-bound proteins, led to an assignment of the observed signal to the $[4Fe4S]^{3+/2+}$ couple utilized by HiPIPs rather than the $[4Fe4S]^{2+/1+}$ couple favored by ferredoxins.

To understand how this redox activation occurred, it was necessary to directly compare the redox potential of the [4Fe4S] cluster in the presence and absence of DNA. The DNA-dissociated [4Fe4S] enzymes were previously shown to be resistant to a change in cluster redox state even in the presence of powerful chemical oxidants *(3)*. This redox insensitivity suggested that the DNA-dissociated proteins have high reduction potentials outside the physiological range, requiring an electrode with a wider available potential window than gold. The 2V scanning window of highly-oriented pyrolytic graphite (HOPG) satisfied this requirement, and it could furthermore be modified with DNA by appending a pyrene linker to the end of the duplex to form a non-covalent bond with the surface (*22*). On the bare electrode, CV and SQWV revealed an irreversible signal for EndoIII with an oxidative peak centered at 250 mV versus NHE, just outside the physiologically relevant potential range (Figure 1.3). An irreversible $[4Fe4S]^{2+/1+}$ reduction was also observed around -300 mV, supporting the initial assignment of the DNA-

bound signal to the $[4Fe4S]^{3+/2+}$ couple. In the presence of DNA, however, the $[4Fe4S]^{3+/2+}$ couple underwent a shift in potential of ≥ -200 mV and became much larger and more reversible; signal loss in the presence of an abasic site confirmed that this process was DNA-mediated (Figure 1.3). The potential shift, in turn, corresponded thermodynamically to an increase in DNA binding affinity of 3 orders of magnitude for the oxidized $[4Fe4S]^{3+}$ form of the protein, relative to the reduced $[4Fe4S]^{2+}$ form. The lack of significant conformational differences between the DNA-dissociated and DNA- bound structures of EndoIII and MutY (*16, 23*) suggested that this potential shift is due to the electrostatic effects resulting from binding to the polyanionic backbone of DNA; the DNA polyanion tunes the potential of the bound [4Fe4S] cluster. More recent results examining EndoIII and MutY along with electrostatic mutants in electrochemistry experiments on graphite support this notion, and are the topic of Chapters 2 and 3 (*24*). In addition, limitations to the HOPG system and their solutions are discussed in detail in Chapter 2.

Overall, these electrochemical experiments revealed several critical details about the redox properties of [4Fe4S] proteins in BER. First, DNA binding activated the proteins for redox activity under physiological conditions by negatively shifting the potential, and this negative shift meant that the oxidized form of the protein would necessarily bind DNA with a much greater affinity than the native, reduced form. Second, EndoIII, MutY, and UDG all displayed DNA-mediated redox signals centered around 85 mV vs. NHE, and thus similar DNA-bound redox potentials for the cluster. With no other obvious redox partners, it was reasonable to consider whether these DNA-bound enzymes might be using DNA CT to signal to each other. CT between even distant DNA-bound proteins is certainly temporally feasible, as DNA charge equilibration takes place on the nanosecond timescale (*25*) while proteins diffuse along DNA on the microsecond to millisecond timescale.

One clear partner for redox chemistry was the guanine radical. Under conditions of oxidative stress, guanine radicals are generated in the DNA duplex, and indeed MutY recognizes and repairs 8-oxoguanine/A mismatches, generated after the formation of oxidized guanine radicals in DNA. Guanine damage generated by long-range oxidation of guanine through DNA-mediated CT has been measured biochemically and occurs over long molecular distances (*26,27*)**.** Monitoring guanine radical formation spectroscopically was used to determine rates of DNA CT; DNA CT occurs on the nanosecond timescale and is rate-limited by the base pair motions (*25*). In fact, EPR and transient absorption spectroscopies were used to characterize DNA CT between the guanine radical and MutY, resulting in formation of the oxidized $[4Fe4S]^{3+}$ cluster (*28*). We have also demonstrated that guanine radicals can transcriptionally activate SoxR from a distance (*29*). SoxR is an iron-sulfur protein that acts as a sensor of oxidative stress in bacteria and activates a series of genes to respond to the stress **(**Figure 1.4**)**. Thus, under conditions of oxidative stress, it is likely that the guanine radical can be a source for oxidation of the BER enzymes with [4Fe4S] clusters by DNA CT and a means potentially to signal the need to activate necessary repair.

The fact that cellular DNA is not linear but wrapped around histones in chromatin brought up an important concern about the feasibility of long-range signaling *in vivo*: can DNA CT still occur in DNA wrapped around histones in a nucleosome core particle? This issue was addressed by an experiment that isolated DNA cleavage at sites of guanine oxidation in nucleosome-wrapped DNA using a rhodium photooxidant covalently tethered to one end of the DNA (*30*). The occurrence of damage, even at sites distant from the photooxidant, demonstrated that curvature of the DNA is unimportant as long as local π-stacking is unperturbed. The wrapping of DNA around histones produces very gradual curvature, not the kinking of DNA,

which is known to interfere with DNA CT. Local π-stacking perturbations can arise from the binding of certain proteins, as has been shown with the transcription factor TATA binding protein, which kinks the DNA duplex at a sharp angle and effectively shuts off CT (*31*). This is not, however, the typical binding mode of DNA-binding proteins; helix-turn-helix proteins do not interfere with DNA CT and thus many proteins that coat the DNA in the cell are not expected to affect long range signaling through DNA CT.

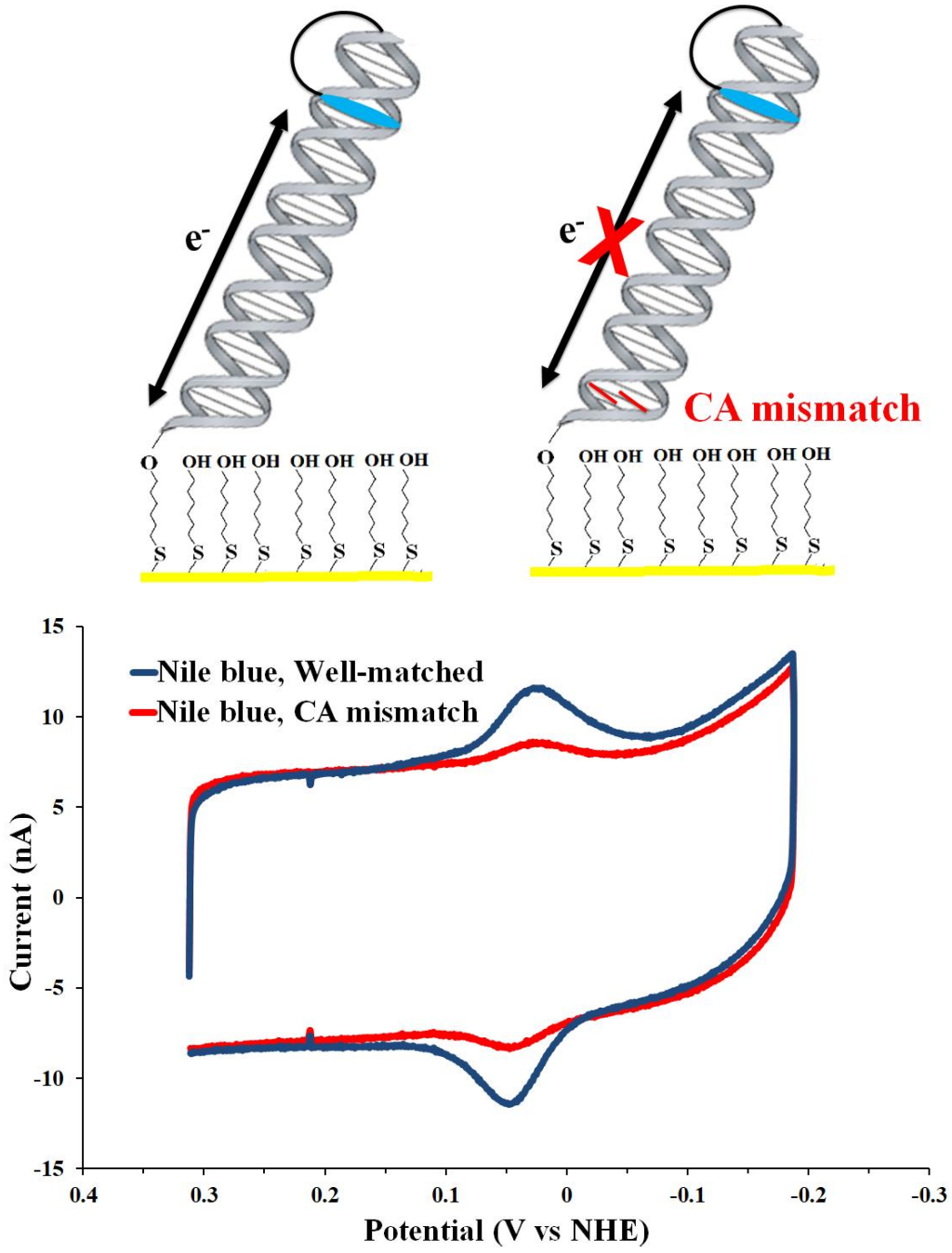

Figure 1.1 Redox probe electrochemistry on DNA-modified gold electrodes. As illustrated by Nile blue, DNA-intercalating redox probes can participate in DNA-mediated charge transport on this platform to produce a reversible signal by cyclic voltammetry (CV; blue). The presence of a single modest disruption, such as a CA mismatch, markedly attenuates CT (red).

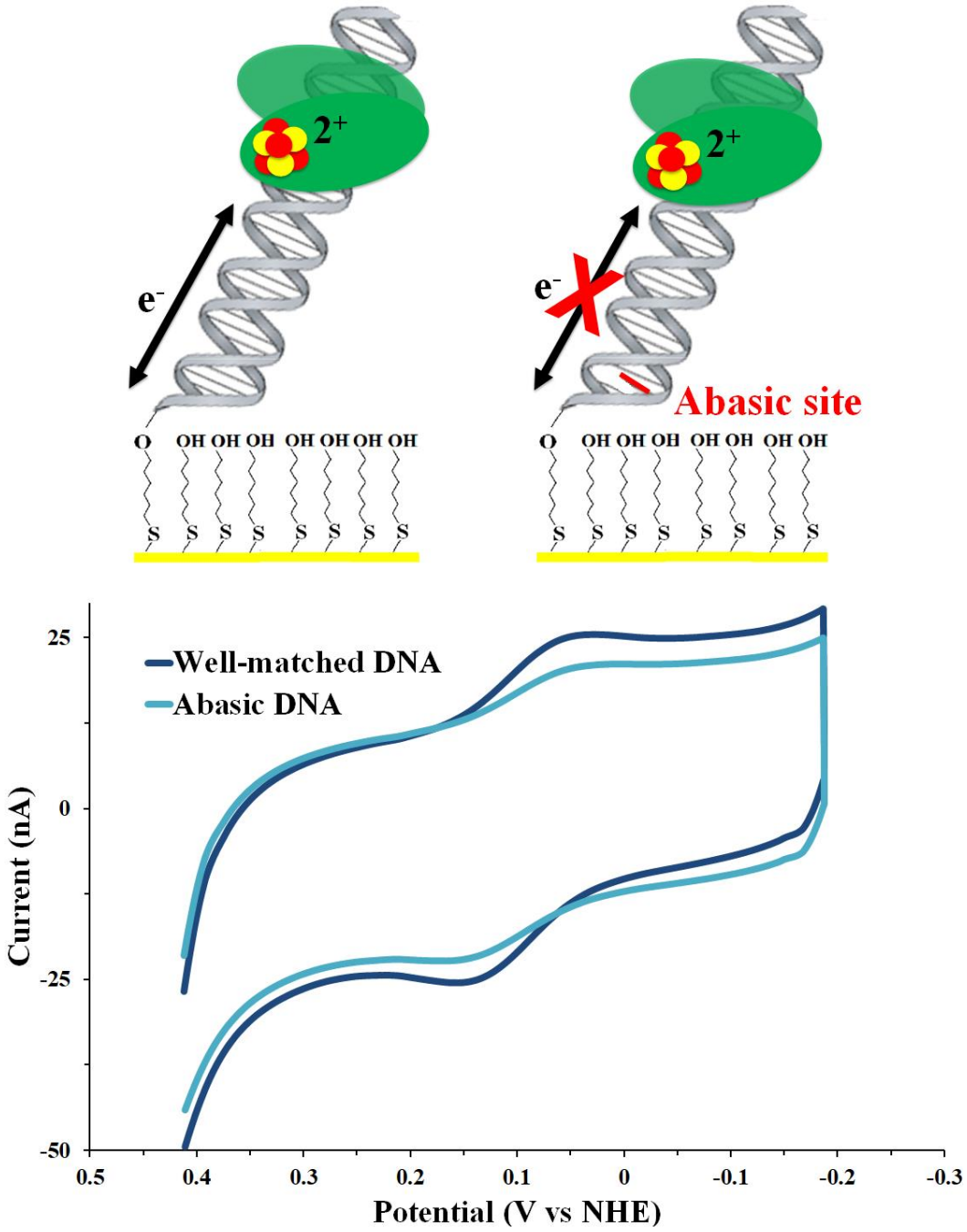

Figure 1.2 Protein electrochemistry on DNA-modified gold electrodes. When a [4Fe4S] cluster protein binds to DNA on a self-assembled monolayer, electron transfer between the cluster and the electrode is highly efficient (left cartoon, dark blue CV). If an abasic site or mismatched base pair is incorporated into the DNA sequence, CT is disrupted and the signal is effectively shut off (right cartoon, light blue CV).

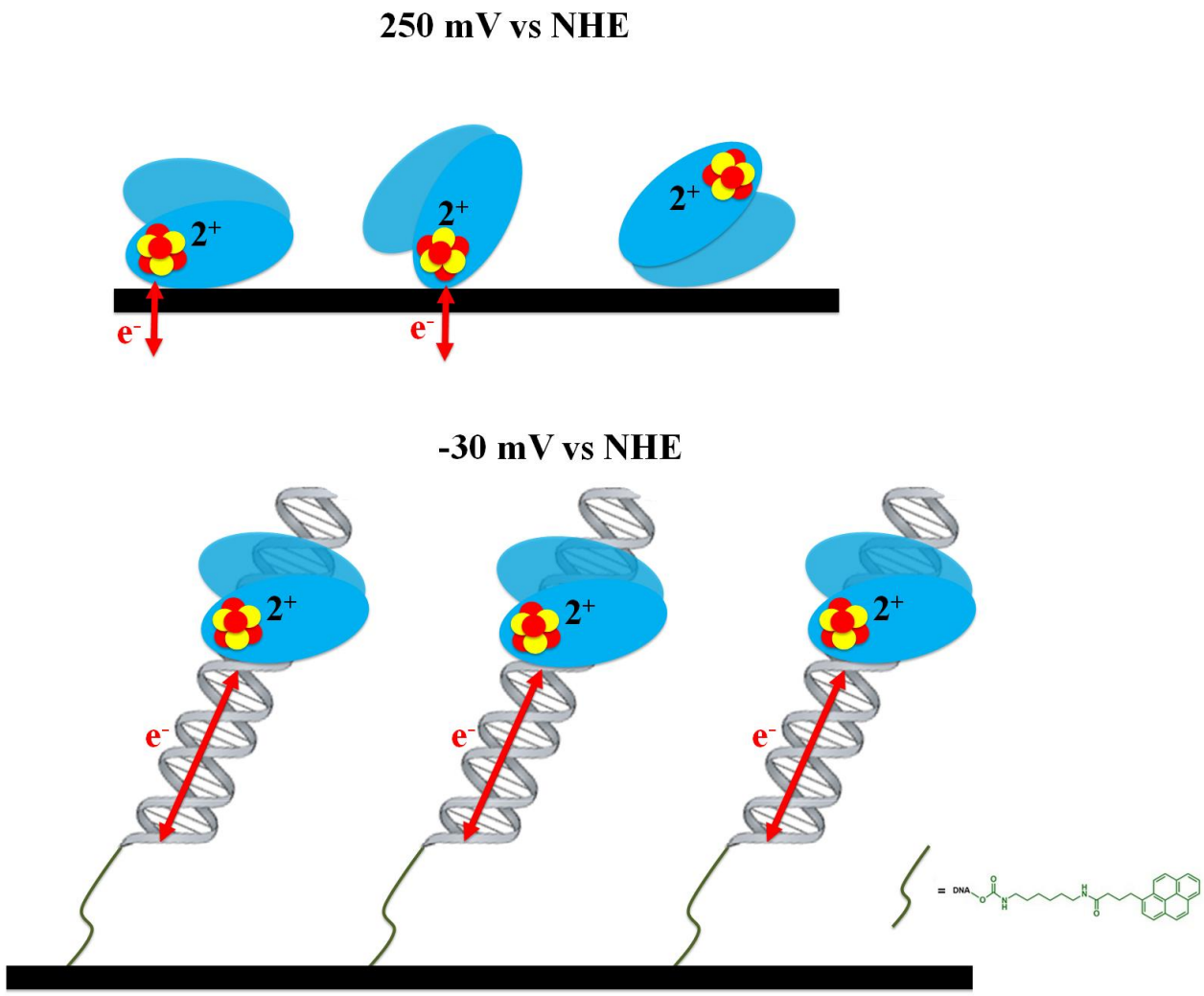

Figure 1.3 EndoIII electrochemistry on a highly oriented pyrolytic graphite (HOPG) electrode in the presence and absence of DNA. When EndoIII was incubated in solution on HOPG, an irreversible signal with a potential of 250 mV vs NHE by square wave voltammetry was observed (top). Importantly, the $[4Fe4S]^{2+/1+}$ couple could also be observed around -300 mV vs NHE, in agreement with the assignment of the high potential couple to the $[4Fe4S]^{3+/2+}$. In contrast, when a film of pyrene-modified DNA was present, the EndoIII signal was reversible and the potential shifted over 200 mV to -30 mV vs NHE (bottom). Due to the lack of significant conformational changes upon DNA binding, this effect was attributed primarily to the electrostatic effects associated with binding to the polyanionic DNA backbone.

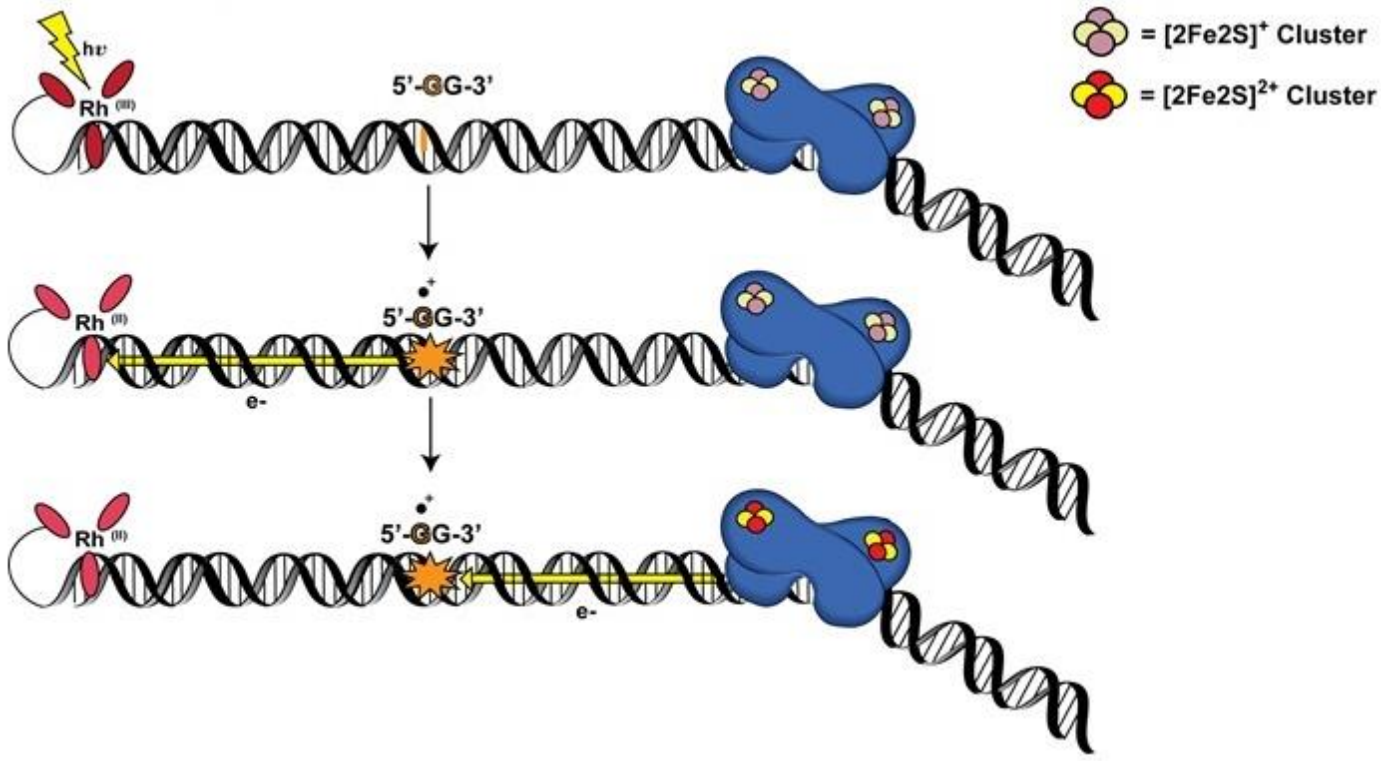

Figure 1.4 Transcription factor SoxR, activated in response to oxidative stress in the cell, contains a [2Fe2S] cluster, which is oxidized from the $[2Fe2S]^{+}$ form to the $[2Fe2S]^{2+}$ form when turned on for activity. Using a DNA-intercalating Rh (III) photooxidant, a guanine radical is generated at the 5′- position in a 5′-GG-3′ doublet. The guanine damage can be repaired at a distance by bound SoxR, though DNA CT. The guanine damage in turn oxidizes SoxR to the $[2Fe2S]^{2+}$ form and turns on the oxidative stress response.

Assessing redox signaling by [4Fe4S] proteins *in vitro* and *in vivo*

In addition to exploring chemically whether the [4Fe4S] cluster of the repair proteins could be oxidized in a DNA-mediated reaction, we became interested in visualizing the process. To do so, an atomic force microscopy (AFM) assay was developed to assess the distribution of [4Fe4S] proteins on DNA (Figure 1.5, ref. *32*). Specifically, this assay involved the addition of WT EndoIII to a mixture consisting of a 3.8 kb DNA substrate, either completely well-matched (WM) or containing a single CA mismatch (MM), and two smaller (2.2 and 1.6 kb) strands of WM DNA (from which the larger strand was composed). This solution was dried on a mica surface and imaged, with DNA-bound proteins distinguished by their greater height relative to DNA and free proteins, thereby providing a visual snapshot of the equilibrium binding distributions of proteins on the DNA. With respect to the distribution, it was predicted that redox signaling would cause tightly bound oxidized proteins to be trapped in the vicinity of a CT-attenuating mismatch, leading to an increase in binding density on mismatched DNA over well-matched DNA. The notion is that on the well-matched strand, there is extensive DNA-mediated CT between the DNA-bound proteins, facilitating the dissociation (with reduction) and reassociation (with oxidation) of proteins onto different strands. With a mismatch on the strand, DNA CT is inhibited, and thus little dissociation and redistribution occurs, leading ultimately to proteins being bound preferentially on the mismatched versus fully matched duplexes. Importantly, a CA mismatch is not a substrate for EndoIII, so there is no intrinsic reason for the proteins to localize to this strand. Indeed, we found that EndoIII binding density ratios for WM versus MM DNA (proteins bound per kb on long DNA/proteins bound per kb on short DNA) averaged to 1.6 for mismatched long DNA, indicating a preference for mismatched strands. In

control experiments where the long and short strands were both fully matched, the binding densities were always essentially the same.

Although EndoIII as purified is largely in the $[4Fe4S]^{2+}$ oxidation state, enough $[4Fe4S]^{3+}$ EndoIII must be present in a given sample to allow redistribution in the AFM assay. However, EndoIII and other BER proteins generally operate under conditions of oxidative stress in which one would expect a higher proportion of the proteins to be oxidized. To test conditions in which more oxidized $[4Fe4S]^{3+}$ protein is initially present, EndoIII/DNA mixtures were incubated with hydrogen peroxide prior to AFM imaging (*32*). Consistent with oxidative stress activating this process, oxidation resulted in an increase in the redistribution, with the binding density ratio on mismatched DNA increasing from 1.6 to 2.4. The protein is able to "find" the strand containing a single mismatch on a 3.8 kilobase duplex.

EndoIII mutants that were defective in carrying out DNA CT had been prepared and characterized, and it was of interest to see how these mutations would affect redistribution. Tyrosine and tryptophan residues are well known to facilitate electron transfer within proteins (*33*), and it was reasonable to consider that they might be involved in relaying electrons between DNA and the cluster in EndoIII. With this aim, a range of mutants were prepared and characterized in activity assays, and their CT properties were then investigated in electrochemical experiments and the AFM assay (*34*). Independent mutation of several aromatic residues in EndoIII, including F30, Y55, Y70, and Y82, resulted in proteins with full catalytic activity and an identical midpoint potential but differing extents of CT deficiency relative to WT, as measured by the current signal height per cluster in a cyclic voltammogram on a DNA electrode. Interestingly, we could correlate directly the efficiency of DNA CT with redistribution in the AFM assay; those proteins which showed poor electrochemical signals on DNA

electrodes, reflecting poor DNA CT, also showed low binding density ratios in the AFM assay, while those with high DNA CT efficiency showed high ratios for redistribution onto the mismatched strand. Thus proteins with efficient DNA CT could more effectively find the mismatched strand.

But does this signaling occur within the cell? To see if these redox-based exchanges between [4Fe4S] proteins occur in the cell, we took advantage of a genetic assay, our "helper function" assay designed to assess the effect of CT signaling on MutY activity (Figure 1.6, ref. *32*). This assay used *E. coli* strain CC104, which has a cytosine swapped for an adenine in the *lacZ* Glu-461 codon, preventing β-galactosidase activity and inhibiting growth in media with lactose as the primary carbon source. Because MutY specifically removes adenine mispaired with oxo-guanine, lowered MutY activity in the CC104 strain results in CG → AT transversions that restore β-galactosidase activity and growth on lactose (lac^+). Numbers obtained could range from ~20 revertants per 10^9 plated cells in the background to over 300 revertants per 10^9 cells when MutY was knocked out. To see if cooperation or signaling with other [4Fe4S] proteins might affect MutY activity, the EndoIII gene (*nth*) was knocked out in the CC104 strain; critically, EndoIII does not resolve A-oxoG mispairs, so it cannot function redundantly with MutY. Despite this, nth^- cells showed an average of 54 lac^+ revertants, more than a two-fold increase over background, indicating that EndoIII "helps" MutY find its targets. To verify that this effect was due to long range CT, CC104 nth^- strains were complemented with plasmids encoding either CT-deficient EndoIII Y82A or catalytically inactive but CT-proficient D138A. Y82A was unable to restore background transversion rates, which were indistinguishable from uncomplemented nth^-; in contrast, D138A, despite its inability to carry out the glycosylase reaction, was able to help MutY and lower transversion rates to background levels. These genetic

results provided a direct link between DNA CT and the observed ability of EndoIII to assist MutY in finding its targets.

These assays thus laid a foundation for considering how long range signaling through DNA CT might indeed function for communication and cooperation among [4Fe4S] cluster repair proteins within the cell. In our model, DNA repair proteins with [4Fe4S] clusters use long-range redox signaling to communicate on DNA as a first step in locating their targets (*32*). As illustrated in Figure 1.7, a redox-inert repair protein in the native $[4Fe4S]^{2+}$ oxidation state binds to DNA and becomes activated toward oxidation. If another distally bound protein is in the oxidized $[4Fe4S]^{3+}$ state, the newly-bound protein can reduce it at a distance via DNA CT; upon reduction, the binding affinity of the distal protein is lowered and the protein is free to diffuse to another region of the genome. When the intervening DNA between the two proteins is undamaged, this self-exchange reaction proceeds efficiently. However, if a mismatch or lesion is present between the proteins, CT is attenuated and the proteins can no longer communicate; both proteins then remain oxidized and bound to the DNA in the vicinity of the lesion, significantly reducing the range over which diffusion must occur and allowing repair of the entire genome on a biologically relevant time scale.

In addition to the novelty of the CT-based damage search, this model was particularly relevant because it presented a solution to the significant problem of how repair proteins manage to locate substrates on a time scale feasible for biological processes. Earlier models generally invoked some combination of one-dimensional and three-dimensional diffusion along DNA to explain this problem (*35*), but these mechanisms alone have been estimated to take far too long (over twice the cell's doubling time) for low-copy number proteins like MutY to search the ~4.5 Mb *E. coli* genome (*32*). If oxidative lesions were rare, this might not be a problem, but roughly

1000 such lesions occur per doubling time (*32*), and the situation is no more favorable in other organisms (*5*). However, when DNA-mediated CT scanning of the genome is factored into this process, the search time is significantly reduced even with short CT distances of ~200 bp, and substantially more so with longer CT distances (*32*). Critically, this mechanism does not preclude diffusional search methods, but instead simply provides a way for proteins to reach the vicinity of a lesion significantly more rapidly, and independent of the many other proteins associated with the DNA; once in the vicinity, diffusion over relatively short (~200 kb) distances would be used to locate and recognize the damaged base.

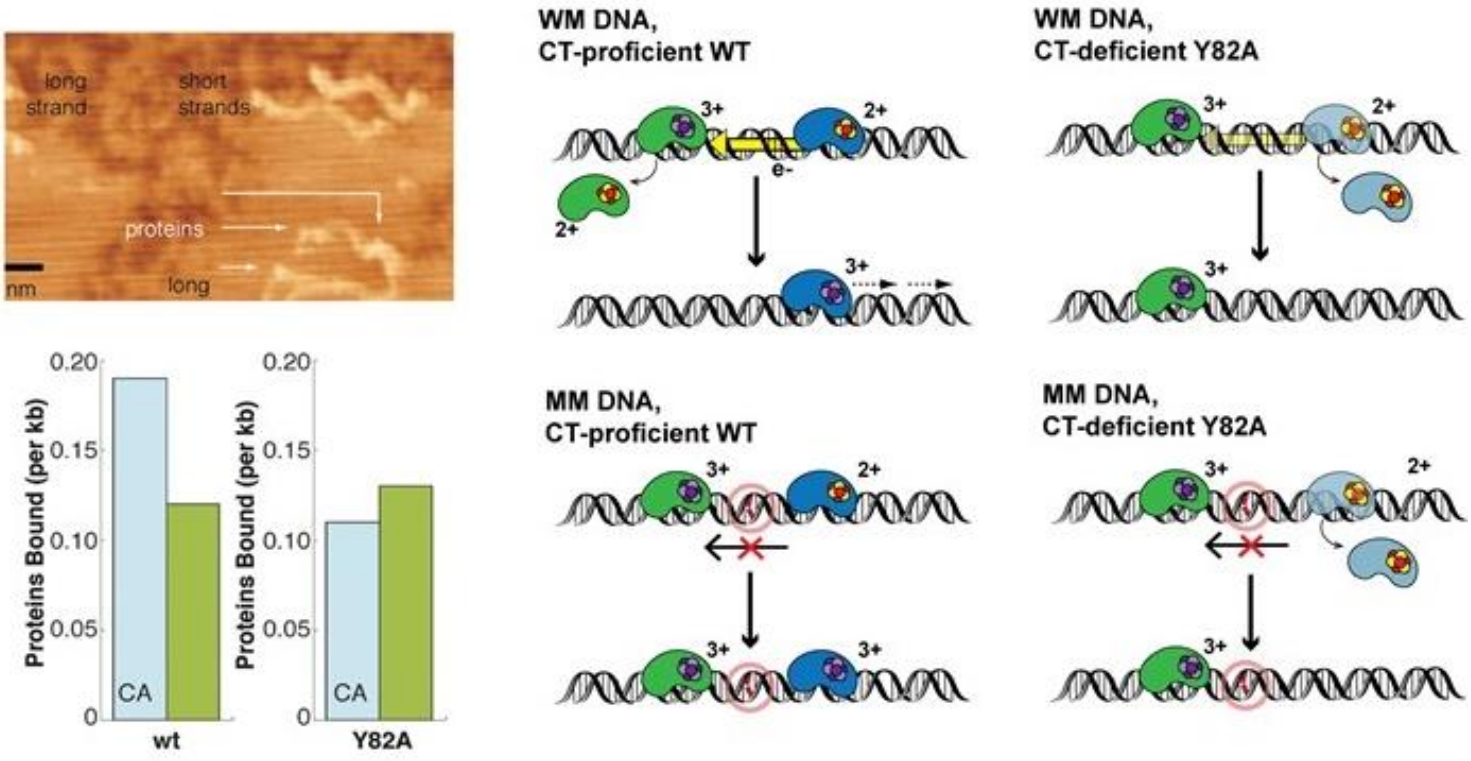

Figure 1.5 Atomic force microscopy (AFM) assay to assess protein redistribution by CT. DNA-bound proteins can be visually distinguished by their relatively great height on the surface, as seen in a sample image at top left. If CT signaling is occurring (middle), WT proteins like EndoIII preferentially bind to DNA containing a CA mismatch, leading to significantly more proteins bound to mismatched strands, as seen in the plot at bottom left. Conversely, when the assay is carried out with a CT-deficient mutant such as EndoIII Y82A (far right), no redistribution is observed (bottom left). Adapted from Reference 32.

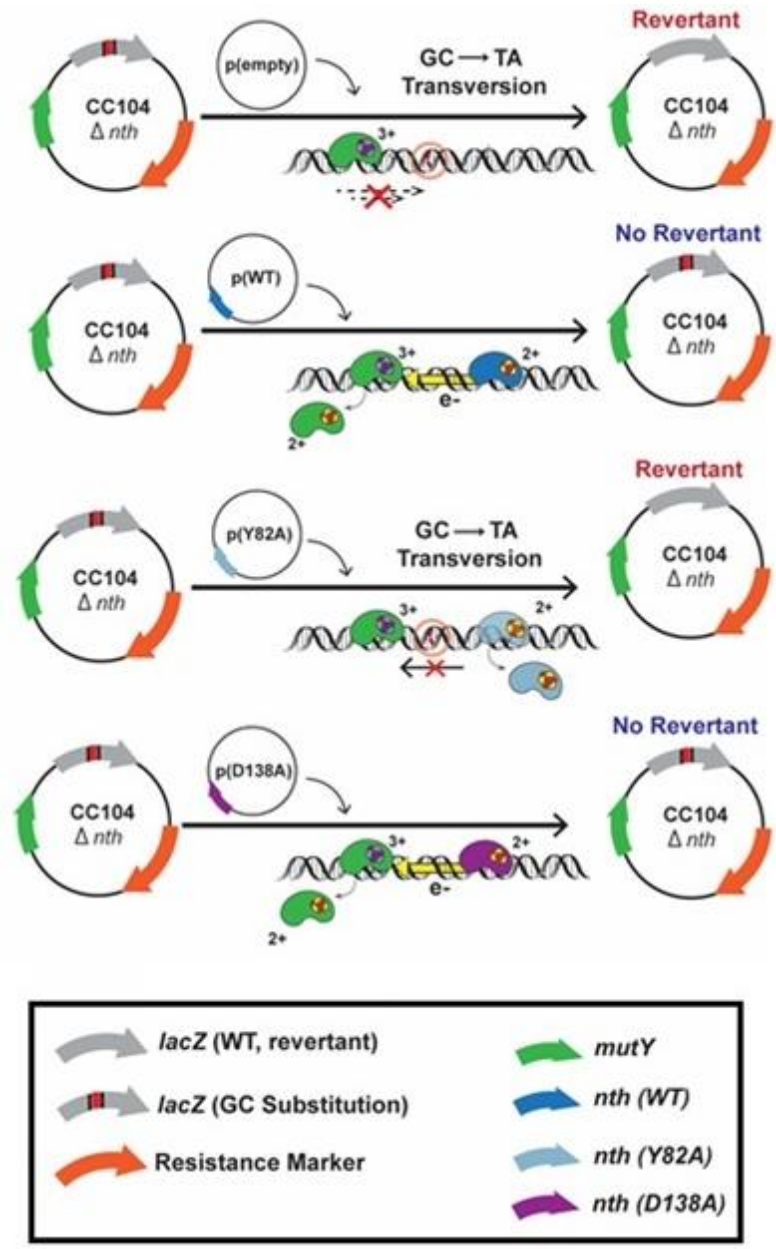

Figure 1.6 *E. coli* helper function assay for MutY activity. The CC104 strain used in this assay contains a GC substitution in the *lac*Z gene, rendering the cells unable to metabolize lactose. Oxidative stress generates 8-oxoguanine, which is readily mispaired with adenine during replication; repair by enzymes that target 8-oxo G ultimately cause a GC → TA transversion, reverting the *lac*Z gene back to WT. MutY, however, excises adenine mispaired with 8-oxoG, so its activity prevents reversions. Remarkably, when EndoIII (nth) is knocked out and an empty plasmid is added in (top), revertants are observed, indicating an impairment in MutY activity. WT EndoIII restores the efficiency of MutY (top middle), while the CT-deficient mutant Y82A is unable to rescue MutY activity (bottom middle). In contrast, the CT-proficient, but catalytically defective, mutant EndoIII D138A has the same restorative effect on MutY activity as WT (bottom), confirming that DNA-mediated redox signaling is the primary factor responsible for this result.

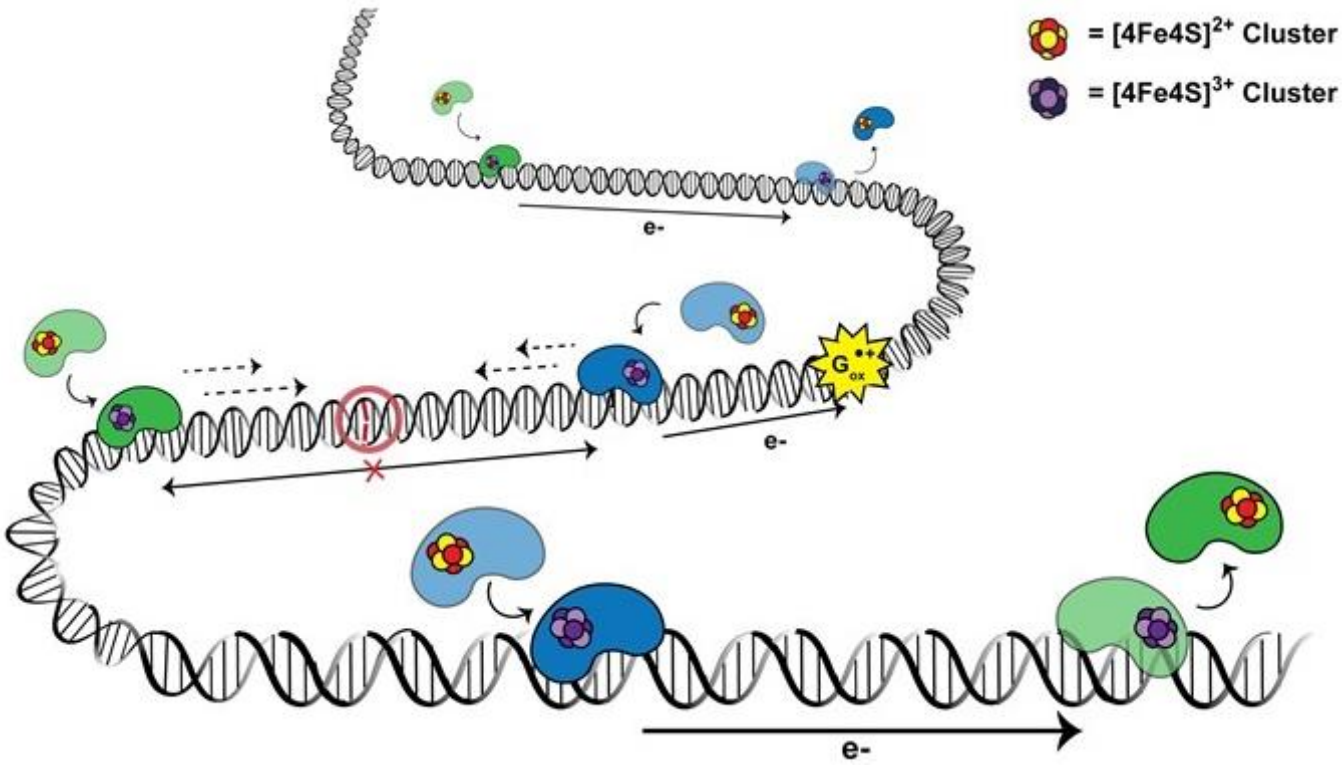

Figure 1.7 A model for DNA-mediated redox signaling between repair proteins. Enzymes with the cluster in the native $[4Fe4S]^{2+}$ first bind DNA, causing the cluster to become activated toward oxidation. Oxidative stress initiates the damage search when highly reactive species such as the guanine radical cation are formed; these can oxidize DNA-bound proteins in their vicinity. Oxidation of the cluster to the $[4Fe4S]^{3+}$ form leads to a 1000-fold increase in DNA binding affinity, so oxidized proteins remain bound and diffuse along the DNA. When another [4Fe4S] protein binds at a distant site, it can send an electron through the DNA base stack to reduce the oxidized protein. At this point, the reduced protein binds less tightly to DNA and diffuses away, while the newly oxidized protein continues the damage search. This process of redox exchange continues until a segment of DNA containing a lesion is approached. Since even subtle lesions can disrupt base stacking, CT is attenuated and any nearby oxidized proteins remain bound. Thus, DNA CT allows repair proteins to scan large sections of the genome and focus their time on areas containing damage.

DNA CT in other repair pathways

In addition to BER, [4Fe4S] proteins have also been found in NER pathways in archaea and, by homology, eukaryotes (*8*). NER involves the removal of bulky lesions such as thymine dimers by exposing the damage through helicase-mediated unwinding of the surrounding ~25 nt of DNA, after which an endonuclease excises the segment and the resultant gap is filled in by a DNA polymerase (*36*). In archaea and eukaryotes, DNA unwinding is dependent upon the ATP-stimulated activity of the [4Fe4S] helicase enzyme XPD. Although XPD is itself part of the transcription factor IIH (TFIIH) complex, it has nonetheless been isolated from the extremophile *Sulfolobus acidocaldarius* and structurally characterized. Upon incubation on a gold electrode modified with an appropriate DNA substrate (20-mer duplex with a 9-mer ssDNA overhang), a reversible, DNA-mediated signal centered at 80 mV vs. NHE is observed (*37*). This signal is comparable in both shape and potential to EndoIII and MutY, in line with predictions for the CT scanning model. In the case of XPD, however, the addition of ATP to stimulate DNA unwinding strongly enhances the current, while the non-hydrolysable analogue ATP γ-S does not. This signal enhancement indicates improved coupling of the cluster to the DNA during activity, a function which could be very important in coordinating with other proteins during NER, effectively "signaling" that the repair protein is functioning.

In humans, mutations in XPD are associated with several diseases, including xeroderma pigmentosum, Cockayne syndrome, and trichothiodystrophy (*8*). The archaeal versions of two of these mutants, G34R and L325V, were characterized electrochemically; both were CT-deficient (*37*,*38*). To see if DNA-mediated signaling could occur between disparate pathways and proteins, *S. acidocaldarius* XPD and *E. coli* EndoIII were incubated together in the presence of DNA and imaged by AFM (*38*). As with experiments involving only EndoIII, the presence of a

CA mismatch resulted in an elevated DNA-binding density ratio; this effect was lost if WT EndoIII or XPD were incubated with a CT-deficient signaling partner, namely XPD L325V or EndoIII Y82A, respectively. Thus, XPD was able to help EndoIII localize to damaged DNA, but only if both proteins were CT-proficient. This experiment established two important general properties of CT between [4Fe4S] proteins: first, that long-range signaling can occur between proteins in distinct pathways, and second, that the proteins do not even have to be from the same organism in order to communicate in this manner. What is critical is that they both bind DNA, have similar DNA-bound redox potentials, and are well coupled into the DNA helix to carry out DNA CT.

E. coli DinG is a superfamily 2 helicase with homology to XPD that also contains a [4Fe4S] cluster (*7*), although DinG is primarily tasked with R-loop maturation rather than NER. R-loop maturation involves the helicase-mediated unwinding of RNA-DNA hybrids that result from collisions between transcription and replication machinery (*39*). We found that DinG behaved similarly to XPD on DNA-modified Au electrodes, displaying a virtually identical midpoint potential, and the increase in current upon the addition of ATP was even more dramatic than for XPD (*40*). Likewise, DinG showed a redistribution onto mismatched DNA in the AFM assay, both alone and in a mixture with WT EndoIII but not when combined with CT-deficient EndoIII Y82A. These assays supported the model developed for CT signaling in repair.

The real value in probing signaling by DinG, as an *E. coli* protein, was the ability to examine *in vivo* signaling in a bacterial system both with EndoIII and MutY. As an initial effort in elucidating signaling between pathways, the *lac*$^+$ helper function assay discussed above was employed to see if CT-active DinG could stimulate MutY activity in the same way as EndoIII. Remarkably, a DinG knockout did cause an increase in *lac*$^+$ reversions, despite the fact that

DinG and MutY are active in distinct repair pathways. This result was in agreement with the *in vitro* AFM studies showing communication between XPD and EndoIII but went further by demonstrating such communication *in vivo* within the same organism.

Importantly, we could ask also if EndoIII signaling was necessary for DinG activity. Here we used the InvA *E. coli* strain to test the effect of EndoIII CT on DinG activity (Figure 1.8, *41*). This assay relied upon the reversal of the frequently transcribed *rrnA* operon in *E. coli* to increase the frequency of replication/transcription collisions, causing stalled forks and generating R-loops; DinG correction of these R-loops was essential for cell survival. Indeed, cell growth was abolished when EndoIII was knocked out, and complementation with either WT or the enzymatically inactive, CT-proficient mutant EndoIII D138A restored survival. In contrast, complementation with the CT-deficient but enzymatically active EndoIII Y82A did not restore survival. Taken together, the MutY helper function and InvA strain survival assays showed that long-range signaling by DNA CT is critical to [4Fe4S] enzymes in disparate pathways: DinG signals BER proteins in their search for damage, and the BER proteins, in turn, can facilitate R-loop resolution by DinG.

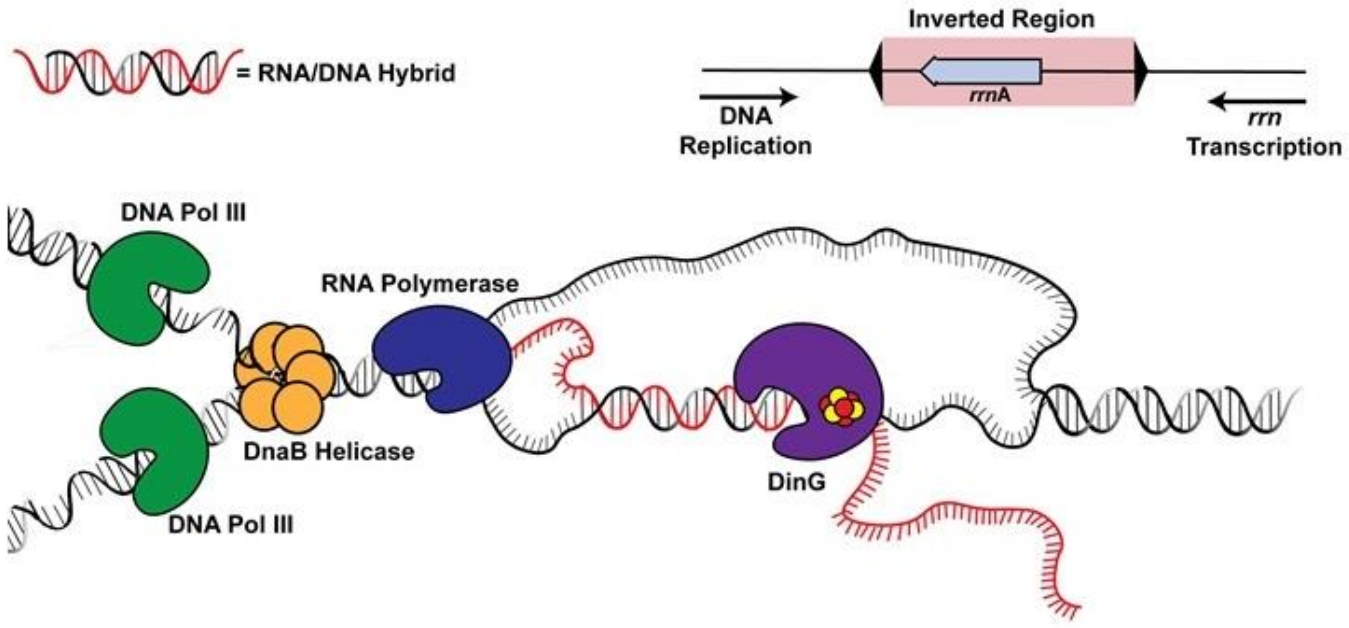

Figure 1.8 *E. coli* inverted A assay for DinG activity. In this assay, the highly transcribed *rrn*A operon has been inverted to increase the rate of replication/transcription collisions, generating R-loops, which the [4Fe4S] helicase DinG unwinds to resolve the stalled fork. Surprisingly, knocking out EndoIII prevented DinG from resolving R-loops, abolishing cell growth. As in the helper function assay (**Figure 1.6**), both WT and the CT-proficient mutant D138A rescued this effect, while CT-deficient EndoIII Y82A did not. Overall, this indicates that CT signaling between EndoIII and DinG is important in helping DinG localize to collision sites.

A role for CT in eukaryotic DNA replication?

In addition to BER and NER, conserved [4Fe4S] clusters have been identified in eukaryotic replication proteins, including yeast and human DNA primase and the yeast B-family DNA polymerases (Pols) α, δ, ε, and ζ (*9-10*) **(**Figure 1.9**).** In DNA replication, a replication bubble is generated by two helicase complexes unwinding DNA in opposite directions, and new DNA strands are synthesized in the 5′ → 3′ direction by DNA polymerases, which extend from a short (8-10 nucleotide) RNA primer generated by a primase enzyme (*42*). The directionality of the polymerases necessitates that one strand, the leading strand, undergoes continuous synthesis in the direction of the fork, and the other, the lagging strand, be formed in discontinuous 120-150 nt Okazaki fragments. Under normal conditions, eukaryotic polymerases divide the task of DNA replication, with Pol α adding 10-20 nt of DNA to the RNA primer before ceding the leading strand to Pol ε and the lagging strand to Pol δ (*43*).

Replication presents an additional puzzle beyond DNA repair, as these proteins do not scan the genome, but instead associate in complexes at replication forks (*44*). Faithful duplication of the genome requires a large amount of coordination among DNA-bound [4Fe4S] proteins, which may be facilitated by DNA-mediated redox signaling. Work in our laboratory has indeed shown this to be the case for DNA primase and the lagging strand polymerase Pol δ (*45*). Primase forms a complex with Pol α (Pol-Prim) *in vivo,* and together these proteins form a 20-30 nt RNA-DNA hybrid primer. The means by which the RNA and DNA segment lengths are precisely controlled, and the mechanism of the primase-Pol α handoff are currently poorly understood. In the case of DNA primase, oxidation of the cluster electrochemically results in markedly enhanced DNA binding, and redox activity has been proposed to act as a switch mediating the hand-off from primase to Pol α. In this model, DNA-bound primase in the

$[4Fe4S]^{3+}$ state would synthesize an 8-10 nt RNA primer, at which point reduction of the oxidized primase by the [4Fe4S] cluster of Pol α would terminate primer synthesis and facilitate the hand-off. Signaling between these particular proteins is a compelling possibility, given that primase and Pol α form a single complex flexible enough to position the [4Fe4S] clusters in primase and Pol α for CT signaling.

Upon completion of the RNA-DNA hybrid primer by Pol-Prim, the primer end is handed off to the clamp loader complex, which attaches the circular sliding clamp PCNA to the primed end; PCNA is then bound by Pol ε on the leading strand and Pol δ on the lagging strand to synthesize long stretches of DNA in a processive manner (*46*). Because the clamp loader does not contain a [4Fe4S] cluster, the Pol δ cluster must have a purpose other than primer handoff. Among other possibilities, a role for the cluster in sensing and coordinating the response to stress during DNA replication was particularly appealing. This intriguing problem led to extensive work with Pol δ, which is described in detail in Chapters 5 through 7.

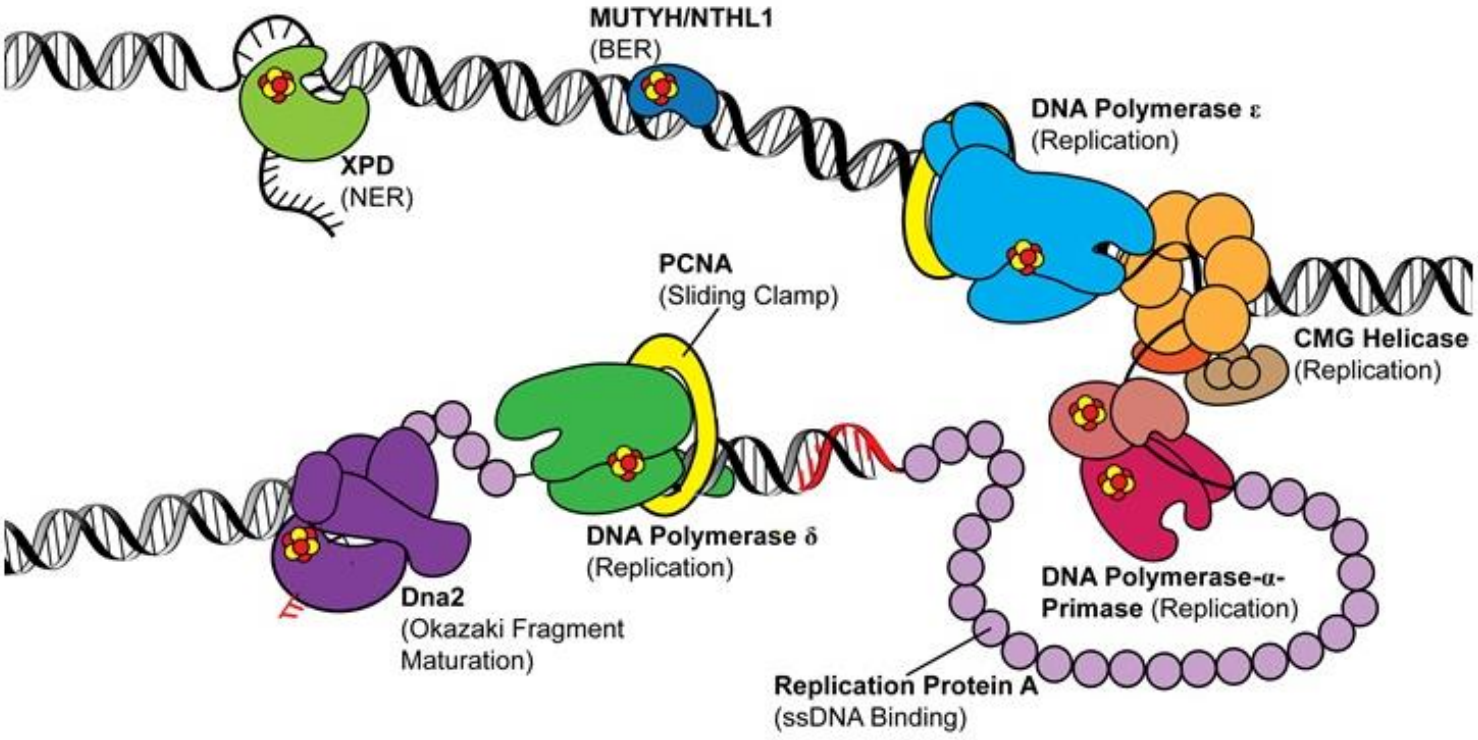

Figure 1.9 DNA-binding eukaryotic enzymes containing [4Fe4S] clusters are found both in replication and in repair pathways. The three polymerases (Polymerase-α-Primase, Polymerase ε, and Polymerase δ) responsible for copying genomic DNA from a parent template all contain a cluster. Polymerase-α-Primase initiates replication through RNA/DNA primer synthesis; Polymerase ε and Polymerase δ then take over replication on the leading and lagging strand of the replication fork, respectively. Dna2 helicase-nuclease, instrumental in Okazaki fragment processing, also contains a [4Fe4S] cluster in its nuclease domain. Repair enzymes, such as XPD helicase in the TFIIH complex (NER) and MUTYH/NTHL1 glycosylases (BER) search for and repair any mismatched/damaged bases on the nascent genomic DNA. This array of [4Fe4S] enzymes in several pathways, with the ability to communicate with one another through DNA CT, suggests that redox signaling may play a larger role in coordinating the complex and dynamic process of eukaryotic replication.

DNA-binding [4Fe4S] proteins in human disease

Many DNA processing proteins containing [4Fe4S] clusters are known to be involved in human disease, with non-catalytic mutations near the cluster being surprisingly prevalent. These proteins include the human homologues of MutY and EndoIII (MUTYH and NTHL1, respectively) and XPD; poorly understood mutations in the [4Fe4S] domain are also present in DNA primase and Pol δ. MUTYH is a critical player in colon cancer, specifically in MUTYH-associated polyposis (*13*). Several poorly characterized mutations in residues near the cluster have recently been recognized. While difficult to understand from conventional perspectives, preliminary electrochemical studies have revealed at least one of these mutants to be more sensitive to oxygen-mediated cluster degradation as described further in Chapter 4 (*48*). Cluster degradation would be especially devastating from the perspective of a CT-based damage search, compromising not only MUTYH but other repair proteins within the redox signaling network. Similarly, NTHL1 has been recognized as important in a variety of different cancers, although mutations in NTHL1 have not been studied to the extent that those in MUTYH have (*14*). XPD mutations are better known for their direct role in three major genetic disorders: trichothiodystrophy, Cockayne syndrome, and xeroderma pigmentosum. These disorders cause a photosensitivity phenotype that ultimately results in the development of cancer and/or accelerated aging. Cancer-relevant mutations in the [4Fe4S] domain have also been reported in both DNA primase and Pol δ (*49, 50*); however, mutations in replicative polymerases are relatively rare due to the essential nature of these enzymes, and those that have been studied generally occur in catalytic domains (*51, 52*). From these examples, it is clear, however, that non-catalytic [4Fe4S] clusters in DNA-processing enzymes are more relevant to disease than

previously suspected. Some work has already implicated defective CT capabilities as important, but many questions remain to be answered.

Conclusions

Our understanding of the role of [4Fe4S] clusters in DNA-processing enzymes has progressed from that of an unusually complex structural group to that of a critical element of rapid, long-range redox signaling along DNA. Considered from another perspective, the recognition of redox-signaling between [4Fe4S] proteins has demonstrated the importance of DNA-mediated CT to biological systems. Indeed, DNA CT is crucial for the identification of lesions by low-copy number proteins like MutY, which would otherwise be unable to find their targets on a relevant timescale. Although this body of work has come a long way toward explaining daunting problems regarding [4Fe4S] proteins and the role of DNA CT in the cell, it opens the door to numerous further questions. These include the nature and origin of the unprecedented potential shift itself, the role of the cluster in disease, and the cluster's function in DNA replication proteins that serve very different purposes than the [4Fe4S] protein studied up to this point.

The work described in following chapters builds upon this basis and represents an effort to answer some of these unresolved questions. This starts with problems in the same bacterial proteins described in this chapter, specifically addressing the role of charged amino acid residues near the cluster in modulating the redox potential and probing the molecular source of the large potential shifts seen on HOPG. Moving beyond bacteria, the role of the cluster in human repair proteins and its relevance to disease was directly addressed for the first time when a remarkable opportunity to study a novel human MUTYH mutation was provided by clinical researchers. Finally, the relevance of clusters in eukaryotic DNA replication, and in the B-family DNA

polymerases in particular, was considered in depth. Indeed, the polymerases, along with DNA primase, represent the first efforts at studying DNA CT in proteins outside of DNA repair. As will hopefully be made clear, despite the diverse functions of these proteins, they all use DNA CT as a regulatory switch to rapidly coordinate activity between pathways and under stress conditions. From a slightly different perspective, this work provides more support for the notion that DNA CT, far from being an esoteric mechanism useful only in detection devices, can serve as a sensor for the integrity of the genome and expedites the cellular response to DNA damage, oxidative stress, and other genomic insults.

References

1) Beinert, H.; Holm, R.H.; Münck, E. Iron-Sulfur Clusters: Nature's Modular, Multipurpose Structures. *Science* **1997**, *277*, 653 – 659.

2) Jacobs, A.L.; Schär, P. DNA glycosylases: in DNA repair and beyond. *Chromosoma* **2012**, *121*, 1 – 20.

3) Cunningham, R.P., Asahara, H., Bank, J.F., Scholes, C.P., Salerno, J.C., Surerus, K., Münck, E., McCracken, J., Peisach, J., and Emptage, M.H. Endonuclease III is an iron-sulfur protein. *Biochemistry* **1989**, *28*, 4450 – 4455.

4) You, H.J.; Swanson, R.L.; Doetsch, P.W. *Saccharomyces cerevisiae* Possesses Two Functional Homologues of *Escherichia coli* Endonuclease III. *Biochemistry* **1998**, *37*, 6033 – 6040.

5) Markkanen, E.; Dorn, J.; Hübscher, U. MUTYH DNA glycosylase: the rationale for removing undamaged bases from the DNA. *Frontiers in Genetics* **2013**, *4*, 1 – 20.

6) Porello, S.L.; Cannon, M.J.; David, S.S. A substrate recognition role for the $[4Fe\text{-}4S]^{2+}$ cluster of the DNA repair glycosylase MutY. *Biochemistry.* **1998**, *37*, 6465 – 6475.

7) Ren, B.; Duan, X.; Ding, H. Redox Control of the DNA-damage inducible Protein DinG Helicase Activity via Its Iron-Sulfur Cluster. *J. Biol. Chem.* **2009**, *284*, 4829 – 4835.

8) Fan, L.; Fuss, J.O.; Cheng, Q.J.; Arvai, A.S.; Hammel, M.; Roberts, V.A.; Cooper, P.K.; Tainer. J.A. XPD Helicase Structure and Activities: Insights into the Cancer and Aging Phenotypes from XPD Mutations. *Cell*, **2008**, *133*, 789 – 800.

9) **a.** Klinge, S.; Hirst, J.; Maman, J.D.; Krude, T.; Pellegrini, L. An iron-sulfur domain of the eukaryotic primase is essential for RNA primer synthesis. *Nat. Struct. Mol. Biol.* **2007**, *14*, 875 – 877. **b.** Weiner, B.E.; Huang, H.; Dattilo, B.M.; Nilges, M.J.; Fanning, E.; Chazin, W.J. An iron-sulfur cluster in the C-terminal domain of the p58 subunit of human DNA primase. *J. Biol. Chem.* **2007**, *282*, 33444 – 33451.

10) Netz, D.J.A.; Stith, C.M.; Stümpfig, M.; Köpf, G.; Vogel, D.; Genau, H.M.; Stodola, J.L.; Lill, R.; Burgers, P.M.J.; Pierik, A.J. Eukaryotic DNA polymerases require an iron-sulfur cluster for the formation of active complexes. *Nat. Chem. Biol.* **2012**, *8*, 125 – 132.

11) Pokharel, S.; Campbell, J.S. Cross talk between the nuclease and helicase activities of Dna2: role of an essential iron-sulfur cluster domain. *Nucleic Acids Res.* **2012**, *40*, 7821 – 7830.

12) Lessner, F.H.; Jennings, M.E.; Hirata, A.; Duin, E.C.; Lessner, D.J. Subunit D of RNA Polymerase from *Methanosarcina acetivorans* Contains Two Oxygen-labile [4Fe-4S] Clusters: Implications for Oxidant-dependent Regulation of Transcription. *J. Biol. Chem.* **2012**, *287*, 18510 – 18523.

13) D'Agostino, V.G., Minoprio, A., Torreri, P., Marinoni, I., Bossa, C., Petrucci, T.C., Albertini, A.M., Ranzani, G.N., Bignami, M., and Mazzei, F. Functional analysis of MUTYH mutated proteins associated with familial adenomatous polyposis. *DNA Repair (Amst)*. **2010**, *9*, 700 – 707.

14) Weren, R.D.A. et al. A germline homozygous mutation in the base-excision repair gene NTHL1 causes adenomatous polyposis and colorectal cancer. *Nat. Genet*. **2015**, *47*, 668 – 671.

15) Thayer, M.M.; Ahern, H.; Xing, D.; Cunningham, R.P.; Tainer, J.A. Novel DNA binding motifs in the DNA repair enzyme endonuclease III crystal structure. *The EMBO J.* **1995**, *14*, 4108 – 4120.

16) Transviña-Arenas, C.H.; Lopez-Castillo, L.M.; Sanchez-Sandoval, E.; Brieba, L.G. Dispensability of the [4Fe-4S] cluster in novel homologues of adenine glycosylase MutY. *FEBS J.* **2016**, *283*, 521 – 540.

17) Netz; D.J.A.; Mascarenhas, J.; Stehling, O.; Pierik, A.J.; Lill, R. Maturation of cytosolic and nuclear iron-sulfur proteins. *Trends in Cell Biol.* **2014**, *24*, 303 – 312.

18) Arnold, A.R.; Grodick, M.A.; Barton, J.K. DNA Charge Transport: from Chemical Principles to the Cell. *Cell Chem. Biol.* **2016**, *23*, 183 – 197.

19) Slinker, J.D.; Muren, N.B.; Renfrew, S.E.; Barton, J.K. DNA charge transport over 34 nm. *Nature Chem.* **2011**, *3*, 228 – 233.

20) Boal, A.K.; Yavin, E.; Lukianova, O.A.; O'Shea, V.L.; David, S.S.; Barton, J.K. DNA-Bound Redox Activity of DNA Repair Glycosylases Containing [4Fe-4S] Clusters. *Biochemistry* **2005**, *44*, 8397 – 8407.

21) Backes, G.; Mino, Y.; Loehr, T.M.; Meyer, T.E.; Cusanovich, M.A.; Sweeney, W.V.; Adman, E.T.; Sanders-Loehr, J. The environment of Fe_4S_4 clusters in ferredoxins and high-potential iron proteins: New information from x-ray crystallography and resonance Raman spectroscopy. *J. Am. Chem. Soc.* **1991**, *113*, 2055 – 2064.

22) Gorodetsky, A.A.; Boal, A.K.; Barton, J.K. Direct electrochemistry of Endonuclease III in the presence and absence of DNA. *J. Am. Chem. Soc.* **2006**, *128*, 12082 – 12083.

23) **a.** Fromme, J.C.; Verdine, G.L. Structure of a trapped endonuclease III-DNA covalent intermediate. *EMBO J.* **2003**, *22*, 3461 – 3471. **b.** Guan, Y.; Manuel, R.C.; Arvai, A.S.; Parikh, S.S.; Mol, C.D.; Miller, J.H.; Lloyd, R.S.; Tainer, J.A. MutY catalytic core, mutant, and bound adenine structures define specificity for DNA repair enzyme superfamily. *Nat. Struct. Biol.* **1998**, *5*, 1058 – 1064. **c.** Woods, R.D.; O'Shea, V.L.; Chu, A.; Cao, S.; Richards, J.L.; Horvath, M.P.; David, S.S. Structure and stereochemistry of the base excision repair glycosylase MutY reveal a mechanism similar to retaining glycosylases. *Nucleic Acids Research* **2015**, *44*, 801 – 810.

24) Bartels, P.L.; Zhou, A.; Arnold, A.R.; Chaffee, N.; Crespilho, F.N.; David, S.S.; Barton, J.K. Electrochemistry of the [4Fe4S] cluster in base excision repair proteins: Tuning the redox potential with DNA. *Langmuir*, **2017**, *33*, 2523 – 2530.

25) O'Neill, M.A.; Becker, H.-C.; Wan, C.; Barton, J.K.; Zewail, A.H. Ultrafast Dynamics in DNA-Mediated Electron Transfer: Base Gating and the Role of Temperature. *Angew. Chem. Int. Ed. Engl.*, **2003**, *42*, 5896 – 5900.

26) Nunez, M.E.; Hall, D.B.; Barton, J.K. Long-Range Oxidative Damage to DNA: Effects of Distance and Sequence. *Chem. Biol. (Oxford, U. K.)*, **1999**, *6*, 85 – 97.

27) Hall, D.B.; Holmlin, R.E.; Barton, J.K. Oxidative DNA Damage through Long Range Electron Transfer. *Nature*, **1996**, *382*, 731 – 735.

28) Yavin, E.; Boal, A.K.; Stemp, E.D.A; Boon, E.M.; Livingston, A.L.; O'Shea, V.L.; David, S.S.; Barton, J.K. Protein-DNA Charge Transport: Redox Activation of a DNA Repair Protein by a Guanine Radical. *Proc. Natl. Acad. Sci. USA* **2005**, *102*, 3546 – 3551.

29) Lee, P.E.; Demple, B.; Barton, J.K. DNA-mediated redox signaling for transcriptional activation of SoxR. *Proc. Natl. Acad. Sci. U. S. A.*, **2009**, *106*, 13164 – 13168.

30) Nunez, M.E.; Noyes, K.T.; Barton, J.K. Oxidative Charge Transport through DNA in nucleosome particles. *Chemistry & Biology* **2002**, *9*, 403 – 415.

31) Gorodetsky, A.A.; Ebrahim, A.; Barton, J.K. Electrochemical Detection of TATA Binding Protein at DNA-Modified Microelectrodes. *J. Amer. Chem. Soc.* **2008**, *130*, 2924 – 2925.

32) Boal, A.K.; Genereux, J.C.; Sontz, P.A.; Gralnick, J.A.; Newman, D.K.; Barton, J.K. Redox signaling between repair proteins for efficient lesion detection. *Proc. Natl. Acad. Sci. USA* **2009**, *106*, 15237 – 15242.

33) Winkler, J.R.; Gray, H.B. Could tyrosine and tryptophan serve multiple roles in biological redox processes? *Philo. Trans. A: Math Phys. Eng. Sci.* **2015**, *373*, DOI: 10.1098/RSTA.2014.0178

34) Romano, C.A.; Sontz, P.A.; Barton, J.K. Mutants of the Base Excision Repair Glycosylase, Endonuclease III: DNA Charge Transport as a First Step in Lesion Detection. *Biochemistry* **2011**, *50*, 6133 – 6145.

35) Verdine, G.L.; Bruner, S.D. How do DNA repair proteins locate damaged bases in the genome? *Chemistry & Biology* **1997**, *4*, 329 – 334.

36) Marteijn, J.A.; Lans, H.; Vermeulen, W.; Hoeijmakers, J.H.J. Understanding nucleotide excision repair and its roles in cancer and aging. *Nature Reviews Mol. Cell Biol.* **2014**, *15*, 465 – 481.

37) Mui, T.P.; Fuss, J.O.; Ishida, J.P.; Tainer, J.A.; Barton, J.K. ATP-Stimulated, DNA-Mediated Redox Signaling by XPD, a DNA Repair and Transcription Helicase. *J. Amer. Chem. Soc.* **2011**, *133*, 16378 – 16381.

38) Sontz, P.A.; Mui, T.P.; Fuss, J.O.; Tainer, J.A.; Barton, J.K. DNA charge transport as a first step in coordinating the detection of lesions by repair proteins. *Proc. Natl. Acad. Sci. USA*, **2012**, *109*, 1856 – 1861.

39) Voloshin, O.N.; Camerini-Otero, R.D. The DinG Protein from *Escherichia coli* Is a Structure-specific Helicase. *J. Biol. Chem.* **2007**, *282*, 18437 – 18447.

40) Grodick, M.A.; Segal, H.M.; Zwang, T.J.; Barton, J.K. DNA-Mediated Signaling by Proteins with 4Fe-4S Clusters Is Necessary for Genomic Integrity. *J. Amer. Chem. Soc.* **2014**, *136*, 16470 – 16478.

41) Boubakri, H.; Langlois de Septenville, A.; Viguera, E.; Michel, B. The helicases DinG, Rep, and UvrD cooperate to promote replication across transcription units *in vivo*. *EMBO J.* **2010**, *29*, 145 – 157.

42) Leman, A.R.; Noguchi, E. The Replication Fork: Understanding the Eukaryotic Replication Machinery and the Challenges to Genome Duplication. *Genes (Basel)* **2013**, *4*, 1 – 32.

43) Lujan, S.A.; Williams, J.S.; Kunkel, T.A. DNA Polymerases Divide the Labor of Genome Replication. *Trends in Cell Biology* **2016**, *26*, 640 – 654.

44) Sun, J.; Shi, Y.; Georgescu, R.E.; Yuan, Z.; Chait, B.T.; Li, H.; O'Donnell, M.E. The architecture of a eukaryotic replisome. *Nat. Strut. Mol. Biol.* **2015**, *22*, 976 – 982.

45) **a.** O'Brien, E.; Holt, M.E.; Thompson, M.K.; Salay, L.E.; Ehlinger, A.C.; Chazin, W.J.; Barton, J.K. The [4Fe4S] cluster in human DNA primase functions as a redox switch using DNA charge transport. *Science* **2017**, *355*, 813. **b.** Bartels, P.L.; Stodola, J.L.; Burgers, P.M.J.; Barton, J.K. A redox role for the [4Fe4S] cluster of yeast DNA Polymerase δ. *J. Am. Chem. Soc.* **2017**, *139*, 18339 – 18348.

46) Georgescu, R.E.; Schauer, G.D.; Yao, N.Y.; Langston, L.D.; Yurieva, O.; Zhang, D.; Finkelstein, J.; O'Donnell, M.E. Reconstitution of a eukaryotic replisome reveals suppression mechanisms that define leading/lagging strand operation. *eLife* **2015**, DOI: 10.7554/eLife.04988

47) Leroy, C.; Mann, C.; Marsolier, M. Silent repair accounts for cell cycle specificity in the signaling of oxidative DNA lesions. *EMBO J.* **2001**, *20*, 2896 – 2906.

48) McDonnell, K.J.; Chemler, J.A.; Bartels, P.L.; O'Brien, E.; Marvin, M.L.; Ortega, J.; Stern, R.H.; Raskin, L.; Li, G.; Sherman, D.H.; Barton, J.K.; Gruber, S.B. A Human MUTYH Variant Linking Colonic Polyposis to Redox Degradation of the $[4Fe4S]^{2+}$ Cluster. **2018**, *Submitted.*

49) Forbes, S.A. et al. COSMIC: mining complete cancer genomes in the Catalogue of Somatic Mutations in Cancer. *Nucleic Acids Res.* **2011**, *39*, D945 - D950

50) Ma, X. et al. Rise and fall of subclones from diagnosis to relapse in pediatric B-acute lymphoblastic leukaemia. *Nat. Comm.* **2015**, doi: 10.1038/ncomms7604

51) Fuss, J.O.; Tsai, C.; Ishida, J.P.; Tainer, J.A. Emerging critical roles of Fe-S clusters in DNA replication and repair. *Biochimica et Biophysica Acta* **2015**, *1853*, 1253 – 1271.

52) Flohr, T.; Dai, J.; Büttner, J.; Popanda, O.; Hagmüller, E.; Thielmann, H.W. **1999**. Detection of mutations in the DNA polymerase δ gene of human sporadic colorectal cancers and colon cancer cell lines. *International J. of Cancer.* **1999**, *80*, 919 – 929.